Supplemental Materials

Molecular Biology of the Cell

Sakane et al.

Supplemental Materials

FIGURE LEGENDS

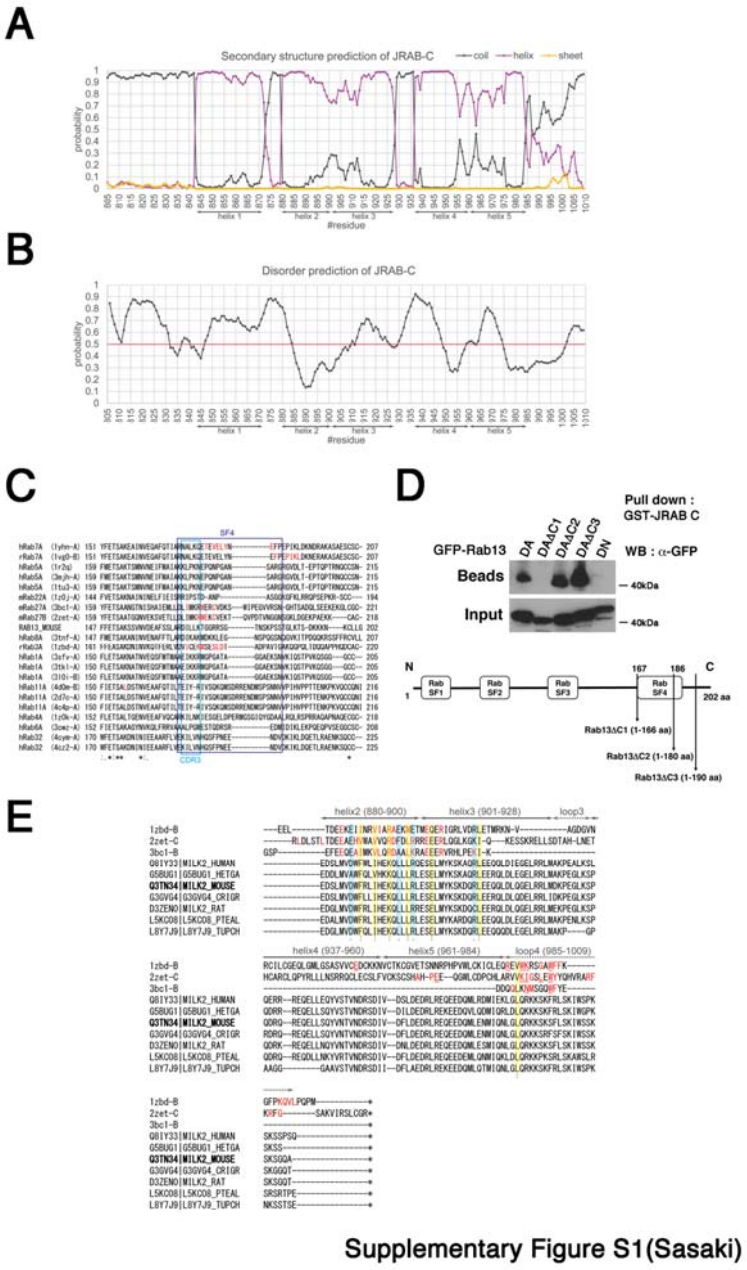

Supplementary Figure S1(Sasaki)

Supplementary Fig S1.Bioinformatic analyses of JRAB-C and Rab13 to resolve the

structure of JRAB-C-Rab13 complex.

(A) Secondary structure of mouse JRAB-C predicted using PSIPRED; the probabilities of random coil, α-helix, and β-sheet regions for each residue are shown by black, pink, and yellow lines, respectively. (B) The probability of a disordered region at each residue in JRAB-C was predicted using POODLE-S. Residueswith a probability greater than 0.5 (above the red line) are considered to be disordered. (C) Sequence alignment of mouse Rab13 with 20 Rab proteins. The structures of 20 Rab–effector complexes were obtained from Protein Data Bank (August 2014). The sequence of mouse Rab13 was aligned with those of Rab in the complexes using ClustalW. In the first column, the first character (h, r, or m) shows the species (human, rat, or mouse, respectively). The effector-binding residues (atomic distance < 4.0 Å) are colored red. This figure shows only the C-terminal region around the CDR3 and SF4 regions of Rab. (D) Upper: HEK293 cells expressing GFP-tagged dominant-active form of Rab13[Rab13DA (aa 1-202)], Rab13DA truncation mutants [Rab13DAΔC1 (aa 1–166), Rab13DAΔC2(aa 1–180), or Rab13DAΔC3(aa 1–190)], or dominant-negative form of Rab13 (Rab13DN) were lysed and subjected to pull-down assays using GST-JRAB-C.

The pulled-down proteins were detected by Western blotting (WB) using an anti-GFP antibody.Lower: Schematic indicates the design of each Rab13DA truncation mutant.Among them, only Rab13DAΔC1 lacks the CDR3(SF4) region.(E) Structural alignment of the three effector proteins, whose structures were derived from those of the corresponding Rab–effector complexes (PDBID: 1zbd, 2zet,and 3bc1), was performed using Mustang; the Rab-binding residues are colored red. A sequence alignment of JRAB/MICAL-L2 in seven species [UniProtID: Q8IY33 (*Homo sapiens*), G5BUG1 (*Heterocephalus glaber*), Q3TN34 (*Mus musculus*), G3GVG4 (*Cricetulus griseus*), D3ZEN0 (*Rattus norvegicus*), L5KC08 (*Pteropus alecto*), and L8Y7J9 (*Tupaia chinensis*)] was generated using ClustalW. Alignment of the effectors with the JRAB C-terminal fragments (corresponding to aa 880–1009 in mouse) was performed by FUGUE. Colored in yellow and cyan are the positions in which the residues in all the sequences share the same property (such as basic, acidic, polar or hydrophobic) and those in which only one residue shows a different property, respectively.

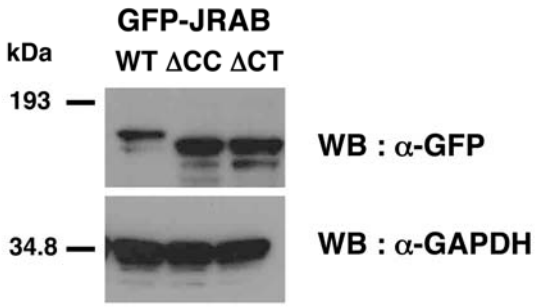

Supplementary Figure S2(Sasaki)

Supplementary Fig S2. Expression level of GFP-JRABwt, GFP-JRABΔCC, or GFP-JRABΔCT in MTD-1A cells. The lysatesof MTD-1A cells stably expressing GFP-tagged JRABwt, JRABΔCC, or JRABΔCT were subjected to SDS-PAGE, followed by WB using either anti-GFP antibody oranti-GAPDH antibody.In this blot, the equal amounts (73μg)of the total protein were loaded.

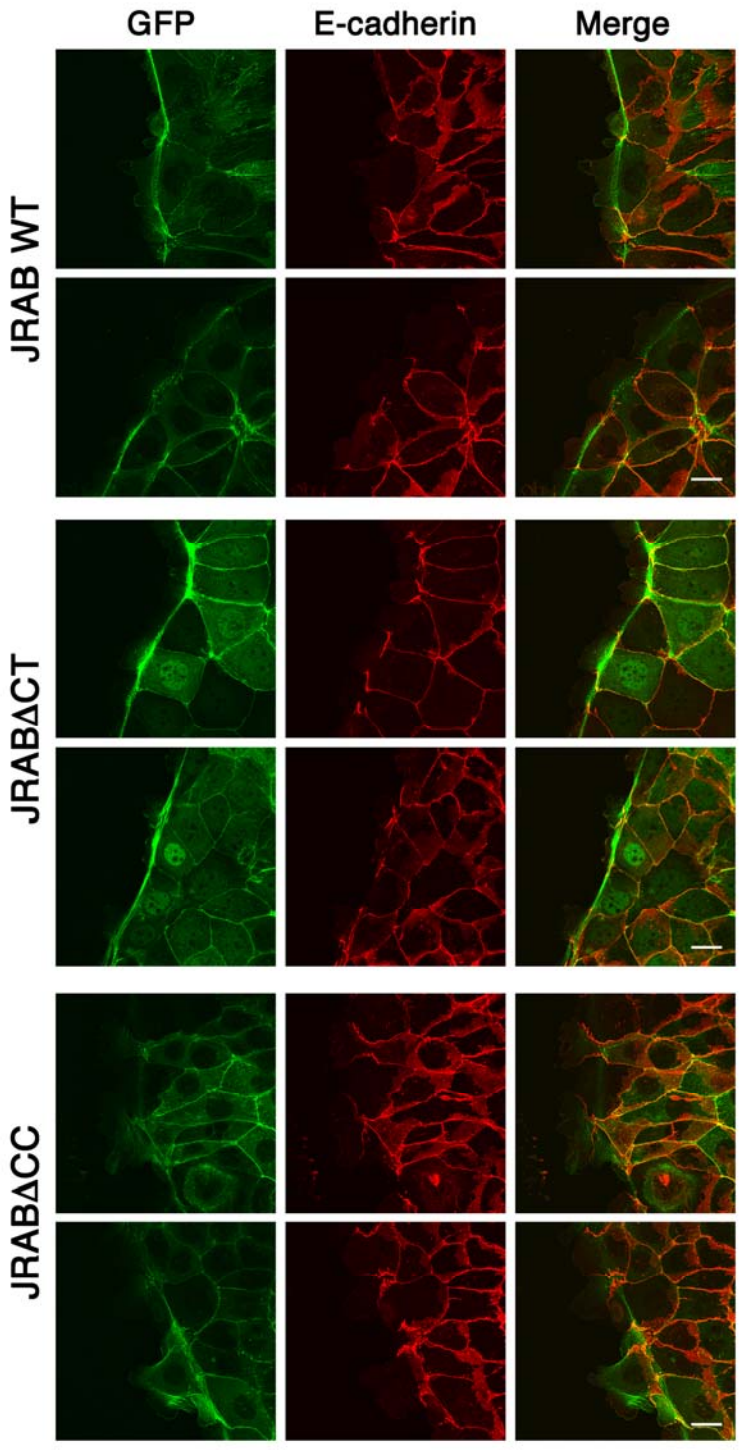

Supplementary Figure S3(Sasaki)

Supplementary Fig S3. Effect of JRAB/MICAL-L2 on the dissociation of adhesion molecule. Confluent monolayers of MTD-1A cells expressing GFP-JRABwt, GFP-JRABΔCT, or GFP-JRABΔCC were scratched, and three hours after wounding,cellswere stained with anti-E-cadherin antibody (red) and observed by confocal microscopy. Scale bar, 20 μm. The results shown are representative of at least three independent experiments and more than twenty fields were observed per experiment.

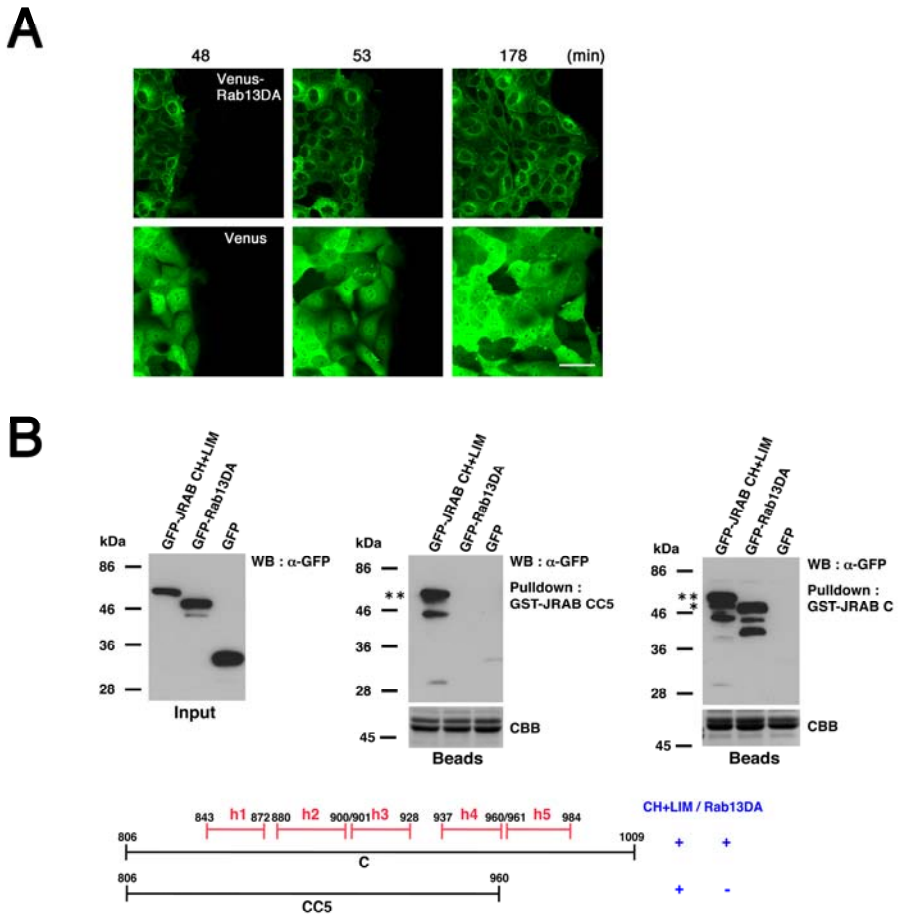

Supplementary Figure S4(Sasaki)

Supplementary Fig S4. Involvement of Rab13 in the conformational change of JRAB/MICAL-L2 in MTD-1A cells.(A) Confluent monolayers of MTD-1A cells expressing Venus-Rab13DA or Venus alone were scratched, followed by observation under a time-lapse microscope for more than 12 hours. Each image was captured at the indicated time (min). Scale bar, 50 μm.(B)HEK293 cell lysatescontainingindicated GFP-tagged JRAB-CH+LIM, Rab13DA, or GFP alone were subjected to pull-down assay using GST-JRAB-CC5(aa 806–960). The pulled-down proteins were detected by WBusing an anti-GFP antibody. The schema indicates JRAB-C and JRAB-CC5, the position of each helix structure (h), and its affinity for Rab13DA or JRAB-CH+LIM. **, GFP-JRAB-CH+LIM; *, GFP-Rab13DA. The amountof purified recombinant protein,GST-JRAB-CC5 or GST-JRAB-C, attached to glutathione-Sepharose beadswas analyzed by SDS-PAGE,followed by CBBstaining. (C) MTD-1A cell lysatescontainingVenus-tagged Rab13DA or Rab13DN were subjected to pull-down assay using GST-JRAB-CC5.The pulled-down protein (open-form JRAB/MICAL-L2) was detected by WB using an anti-JRAB antibody. The amountof GST-JRAB-CC5 attached to glutathione-Sepharose beadswas analyzed by SDS-PAGE, followed by CBB

staining.

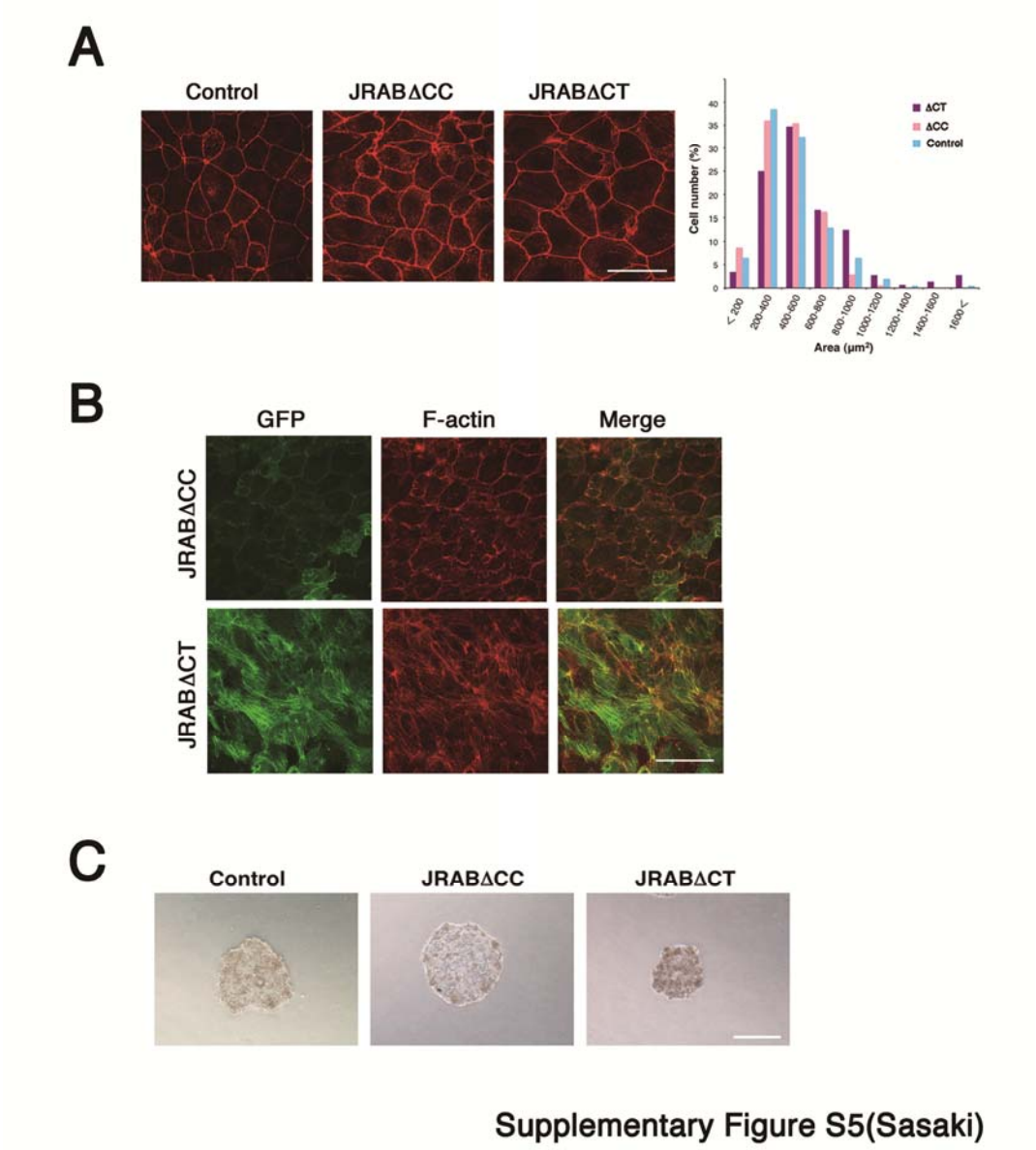

Supplementary FigS5. Inhibition of JRAB/MICAL-L2 conformational plasticity interferes with cell functions.(A) Comparison of cell size following wound healing. (Left) Confocal microscopicimages of cortical F-actin (red) at the junctional level in

MTD-1A cells (Control) and cells expressing GFP-JRABΔCC (JRABΔCC) or GFP-JRABΔCT (JRABΔCT). Scale bar, 50 μm.(Right) The difference among GFP-JRABΔCC (mean ± SD = 448.2 ± 184.6), GFP-JRABΔCT (596.4 ± 315.6), and mock control (466.9 ± 238.2) was quantified ($P = 7.7 \times 10^{-6}$, Kruskal-Wallis analysis of variance). Statistical difference was observed between mock control and GFP-JRABΔCT ($P = 4.6 \times 10^{-5}$) and between GFP-JRABΔCC and GFP-JRABΔCT (P = 6.3×10^{-5}), but not between mock control and GFP-JRABΔCC ($P = 9.9 \times 10^{-1}$) by Steel-Dwass's post-hoc test. Note that cells expressing GFP-JRABΔCT had larger areas at the junctional level than other cell groups.(B)Cells expressing GFP-JRABΔCC or -JRABΔCT were stained with rhodamine–phalloidin (red) and observed by confocal microscopy. Scale bar, 50 μm. The results shown are representative of at least three independent experiments and more than twenty fields were observed per experiment. (C)Representative spheroids, formed in hanging drop culture, of MTD-1A cells (Control) or cells expressing GFP-JRABΔCC or -JRABΔCT. Scale bar, 500 μm.Three experiments were performed independently and more than twenty spheroids were observed per experiment.

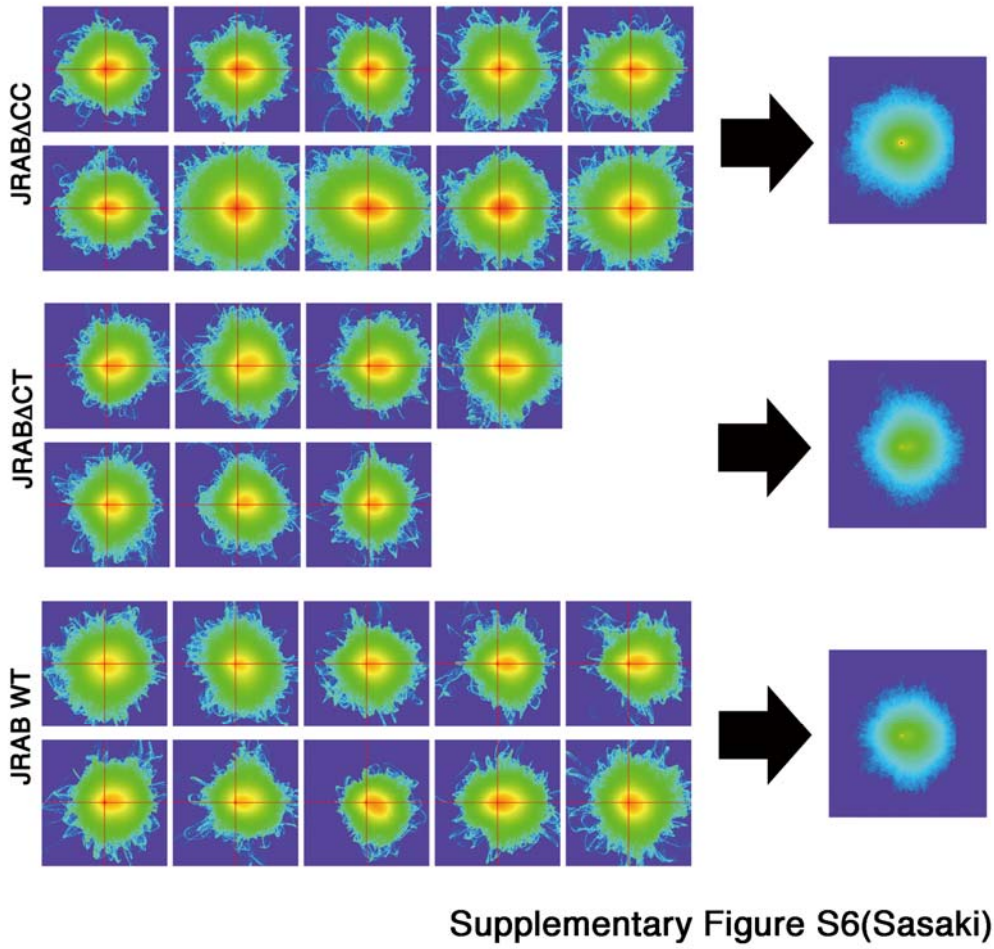

Supplementary FigS6. 2D motion histogram for each dataset and median histogramcorresponding to each population type.

2D motion histograms of JRABΔCC, JRABΔCT, and JRAB WT were prepared from 10, 7, and 10 time-lapse image sets, respectively (left panels). Then, the histograms were converted to a probability distribution by dividing its frequency total, in order to normalize the difference in the time length of the data. The median histogram of each

population type consists of the median values of all normalized motion histograms (right panels).

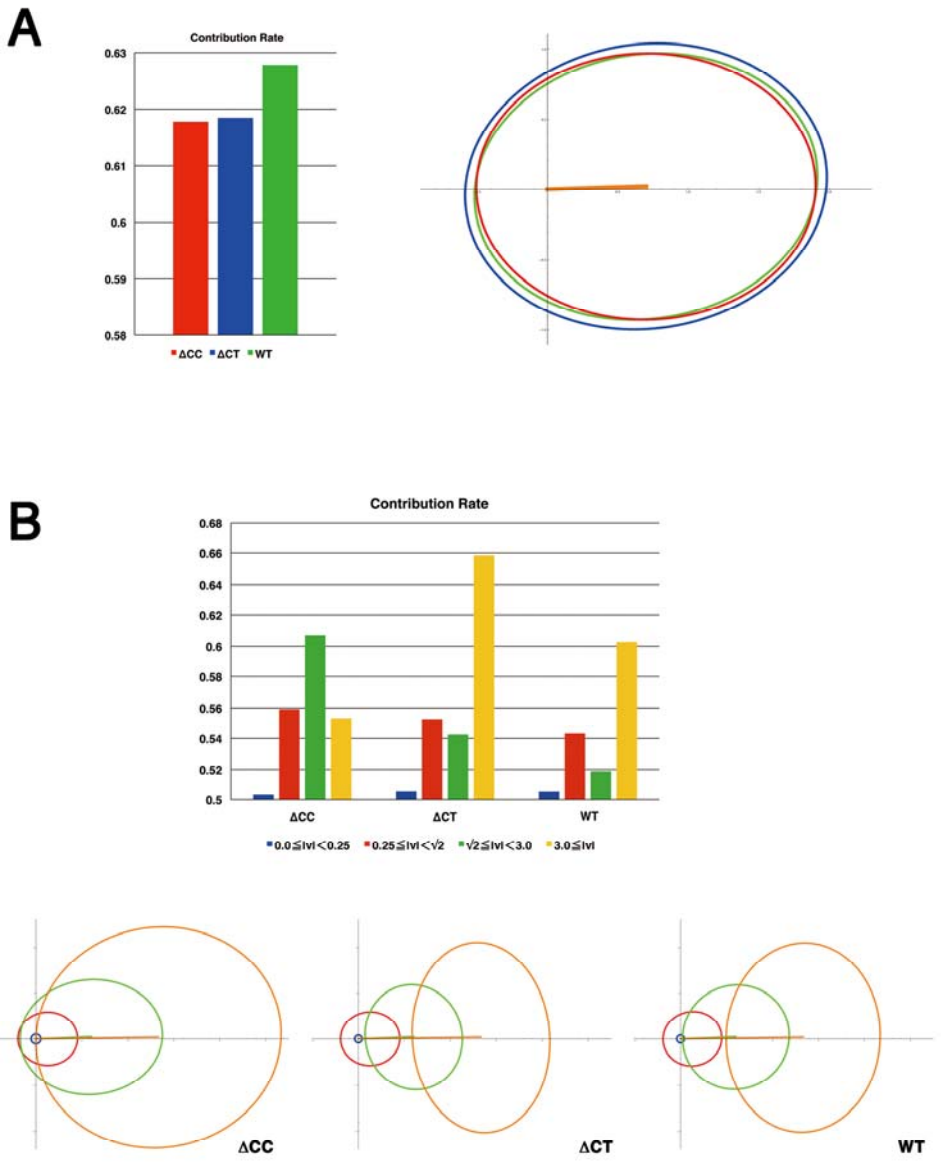

Supplementary Figure S7(Sasaki)

Supplementary FigS7. PCA via average speed vectors over all population types. (A) PCA contribution rate C_r and its corresponding PCA ellipse. Red, GFP-JRASBΔCC; blue, GFP-JRABΔCT; green GFP-JRABwt. (B) PCA contribution rate C_r and its corresponding PCA ellipse within four intervals. $|v|$ is the speed magnitude.Blue, $0 \leqslant |v| \leqslant 0.25$; red, $0.25 \leqslant |v| \leqslant \sqrt{2}$; green, $\sqrt{2} \leqslant |v| \leqslant 8$; yellow, $8 \leqslant |v|$.

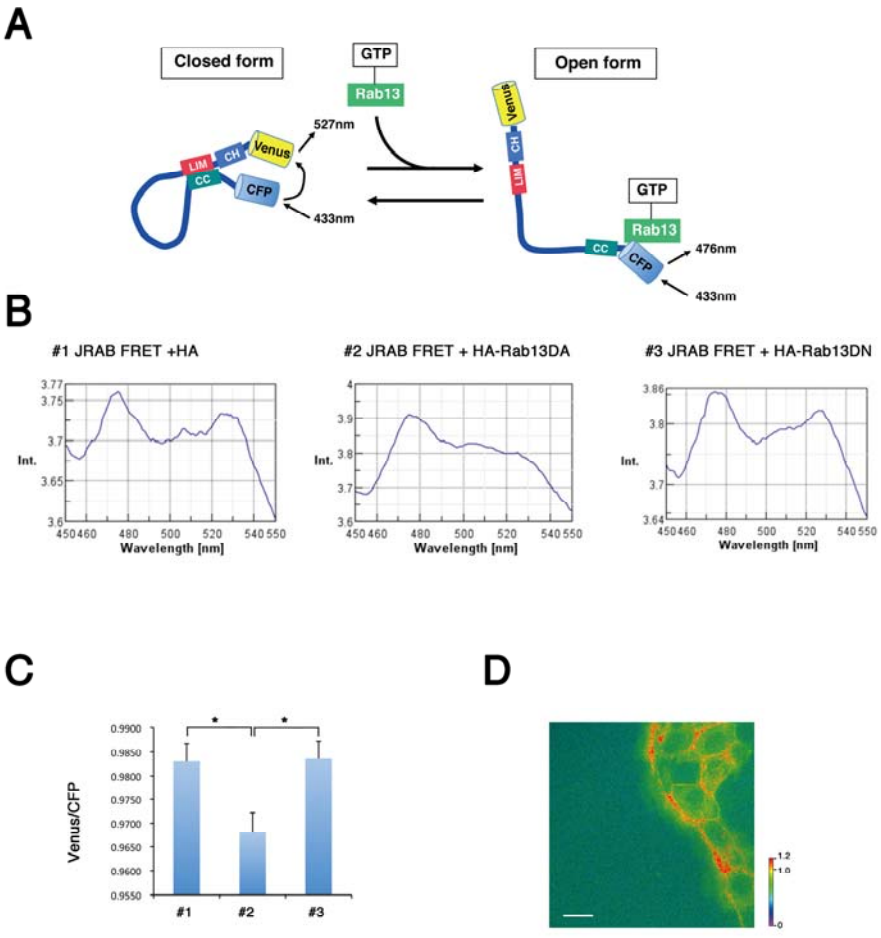

Supplementary Figure S8(Sasaki)

Supplementary FigS8.JRAB/MICAL-L2 changes its conformation depending on the position of the cell within the population.

(A)Proposed model for Rab13-dependent conformational change of JRAB indicator. In closed form, theLIM domain of JRAB/MICAL-L2 interacts with its C-terminal domain. Such intramolecular interaction juxtaposes the N-terminal Venus and

C-terminal CFP, leading to high levels of FRET (excitation at 433nm, emission at 527 nm). Upon binding of GTP-Rab13 (activated Rab13), JRAB/MICAL-L2 adopts the open form and the distance between the N-terminal Venus and C-terminal CFP increases, leading to low levels of FRET (excitation at 433 nm, emission at 476 nm). (B) Activated Rab13–dependent decrease in FRET emission of JRAB indicator. JRAB indicator was expressed in HEK293 cells along with HA, HA-Rab13DA, or HA-Rab13DN, and the level of FRET in cell lysates was measured using a spectrofluorometer. Emission readings at 1-nm intervals were made during excitation at 433 nm. Emission spectra of cell lysates expressing JRAB indicator with HA (#1), with HA-Rab13DA (#2), or with HA-Rab13DN (#3). (C) Emission ratio (Venus/CFP) was averaged and shown here± s.d. (n = 4). Asterisks indicate statistical significance (#1 HA vs. #2 HA-Rab13DA:P = 0.0407;#3 HA-Rab13DN vs. #2 HA-Rab13DA: P = 0.034, ANOVA followed by Tukey's post-hoc test). (D) Confluent monolayers of MTD-1A cells expressing JRAB indicator were scratched. After wounding, cells were imaged by epifluorescence microscopy. Intensity-modulated display (IMD) mode demonstrates high FRET emission at the free edge of the cell population. Scale bar, 20

μm. Video image is shown in Supplementary Video S10.